Index

A

a posteriori probability, 564
Abbe number, 251
aberrations, 250
absorbance, 134
absorption coefficient, 55, 75
absorption cross-section, 75
abundance, 530
abundance matrix, 531
abundance vector, 555
acousto-optic tunable filter (AOTF), 400
adaptive coherence/cosine estimator (ACE), 659
Adaptive Infrared Imaging Spectroradiometer (AIRIS), 398
adaptive subspace detector (ASD), 694
additive model, 507
additivity, 535, 545
adjacency effect, 201, 232
affine transformation, 507
Airborne Hyperspectral Imager (AHI), 357
Airborne Imaging Spectrometer (AIS), 22
Airborne Real-Time Cueing Hyperspectral Enhanced Reconnaissance (ARCHER), 27
Airborne Visible/Infrared Imaging Spectrometer (AVIRIS), 22, 349
Airy radius, 249
albedo, 140
albedo, spherical, 232
algal plumes, 29
allowed transitions, 90
alpha emissivity, 480
alternative hypothesis, 617
angular frequency, 39
anomaly detection, 624
aplanatic, 251
apodization function, 372
apparent spectral properties, 9, 133
argon gas discharge lamp, 420
astigmatism, 250
atmospheric compensation, 451
atmospheric path radiance, 206
atmospheric path transmission, 205
Atmospheric Removal Program (ATREM), 485

B

background spectral radiance, 288
background-limited performance (BLIP), 285
backscatter cross-section, 78
bacteriorhodopsin, 165
bare-soil index (BI), 466
bathymetry, 31
Bayes theorem, 565
Bayesian classification rule, 565

Beard–Maxwell model, 149
Beer's law, 55
beta-carotene, 165
between-class scatter matrix, 571
bidirectional reflectance distribution function (BRDF), 147
biquadratic model, 418
blackbody, 150
blackbody calibration source, 434
blaze angle, 328
Bloch wave function, 129
Bohr radius, 97
Boltzmann's constant, 119
bond strength, 111, 116
Born–Oppenheimer approximation, 90

C

carbon dioxide, 157
carbon monoxide, 119, 158
carbonate, 172
cavity blackbody, 434
cellulose, 169
centering, 514
change detection, 695
characteristic equation, 512
charge velocity, 40
charge-coupled readout device, 266
chi-squared distribution, 627
chlorophyll, 165
Christiansen peak, 178
chromatic aberration, 250
chronochrome, 699
class index, 565
class-conditional probability, 565
class-conditional spectral matched filter (CCSMF), 667
classical mechanics, 45
classification, 546, 564
cluster-based anomaly detector (CBAD), 642
clustering, 546
cold shield, 264
Compact Airborne Spectral Sensor (COMPASS), 354
complementary metal-oxide semiconductor (CMOS), 266
complementary subspace detector, 637
complex dielectric constant, 43, 48
complex index of refraction, 44, 51
complex propagation vector, 43
conductivity, 41
confusion matrix, 568
constant FAR (CFAR), 632
constitutive relations, 41
constrained energy minimization (CEM) detector, 658
correlation diameter, 306
$\cos^4$ law, 290
coupled-subspace model, 492
covariance equalization, 699
covariance matrix, 509
curl, 38
cutoff spatial frequency, 256
cutoff wavelength, 130, 269

D

damping coefficient, 46
damping constant, 49
dark current, 272, 274, 282
data matrix, 504
detection statistic, 619
detector array, 266
detector shunt resistance, 283
deuterium lamp, 431
diagonal matrix, 512
diffraction efficiency, 329
diffuse, 146
diffuse spectra, 128
Digital Image and Remote Sensing Image Generation (DIRSIG), 229

dimensionality, 510
dipole moment, 89
direct solar irradiance, 201
direct thermal emission, 201
directional hemispherical reflectance (DHR), 147
disassociation energy, 116
disaster management, 31
discriminant function, 565
dispersion, angular, 316, 325
dispersion, material, 316
dispersion, prism, 315
distortion, 250
divergence, 38
Doppler broadening, 95
downwelling radiance, 201
Drude theory, 52

E

edge height overshoot, 308
eigenvalue, 512
eigenvector, 512
Einstein coefficients, 92
electric displacement, 40
electric permittivity, 38, 41
electromagnetic radiation, 37
electromagnetic wave, 38
electron charge, 46
electron rest mass, 46
electron volt, 119
electronic charge, 40
emission spectrum, 100
emissive spectral region, 201
emissivity, 153
empirical line method (ELM), 454
endmember, 530
endmember matrix, 531
Euclidean distance (ED), 546
Euclidean distance (ED) detector, 652
exitance, 69
exo-atmospheric solar irradiance, 221
expectation maximization (EM), 596
extinction coefficient, 76
extrinsic photoconductor, 278

F

F distribution, 661
Fabry–Pérot interferometer, 395
false color, 4
false-alarm mitigation (FAM), 674
false-alarm rate (FAR), 622
fast line-of-sight atmospheric analysis of spectral hypercubes (FLAASH), 490
FastICA, 522
feature extraction, 564
field curvature, 250
Field-Portable Imaging Radiometric Spectrometer Technology (FIRST), 387
finite target matched filter (FTMF), 680
Fischer's linear discriminant, 571
fixed pattern noise, 292
f-number, 247
focal plane array (FPA), 243
focal plane spectral irradiance, 289
forbidden transitions, 90
Fourier transform, 368
Fourier Transform Hyperspectral Imager (FTHSI), 391
Fourier transform infrared (FTIR), 363
Fourier transform spectrometer, 20
Franck–Condon factor, 127
free-charge current density, 40
free-charge density, 40
fuzzy cluster-based anomaly detector (FCBAD), 643

G
gaseous effluent model, 233
gaseous effluents, 27
Gaussian mixture model (GMM) detector, 639
Gaussian mixture Reed–Xiaoli (GMRX) detector, 639
gelbstoff absorption, 237
generalized distance formula, 504
generalized image-quality equation (GIQE), 307
generalized likelihood ratio test (GLRT), 623
generation rate, 271
geology, 22
geometric support function, 342
Geosynchronous Imaging Fourier Transform Spectrometer (GIFTS), 388
Gerchberg–Saxton algorithm, 412
grating, 324
grating equation, 325
grating spectrometer, 19
ground-plane radiance, 230
ground-resolved distance (GRD), 301
ground-sampled distance (GSD), 296

H
Hagen–Rubens formula, 191
Hamiltonian, 85
harmonic oscillator, 46, 111
Heisenberg uncertainty principle, 94
hemispherical directional reflectance (HDR), 147
high-resolution transmission molecular absorption (HITRAN), 206
HydroLight, 235
hydroxide, 172
Hyperion, 353
Hyperspectral Digital Imagery Collection Experiment (HYDICE), 351
Hyperspectral Imager for the Coastal Ocean (HICO^{TM}), 31
hyperspectral imaging, 6
hypothesis test, 617

I
ideal geometric image, 247
image registration, 698
imaging spectrometry, 14
improved split-and-merge clustering (ISMC), 586
in-scene atmospheric compensation (ISAC), 468
independent component analysis (ICA), 520
index of refraction, 44
index structure parameter distribution, 306
indicator function, 618
indium antimonide detector, 277
indium gallium arsenide detectors, 276
inherent dimensionality, 526
inscribed simplex, 532
integrated photoelectrons, 291
integrating sphere, 433
intensity, 71
interferogram, 366
internuclear distance, 111
intrinsic spectral properties, 9
irradiance, 69
iterative self-organizing data analysis technique (ISODATA), 584

J
Johnson noise, 284
joint subspace detector, 636

K
k nearest neighbor (kNN), 606

Karhunen–Loeve transformation, 511
Kelly detector, 657
kernel function, 606, 613
kernel trick, 612
keystone, 340
Kirchoff's law, 154
k-means algorithm, 580
Kolmogorov–Smirnov (KS) test, 471
krypton gas discharge lamp, 420
Kubelka–Munk, 139

L
labeling, 564
Lambertian, 72, 146
Landsat, 5
law of reflection, 57
least-angle regression (LARS), 683
lignin, 169
likelihood function, 508
likelihood ratio, 618
likelihood ratio test (LRT), 619
Linde–Buzo–Gray (LBG) clustering, 547, 580
line shape, 94
linear classifier, 567
linear mixing model (LMM), 529
linear variable filter (LVF), 404
load-resistance circuit, 274
local normal model, 540
log-likelihood function, 508
log-likelihood ratio, 619
longwave infrared, 2
Lorentz force, 40
Lorentz model, 46, 49
Lorentzian line-shape function, 94

M
magnetic field amplitude, 38
magnetic induction, 40
magnetic permeability, 38, 41
magnification, 247
Mahalanobis distance (MD), 546, 625
margin, 591
maximum likelihood, 508, 596
maximum noise fraction (MNF) transformation, 518
Maxwell–Boltzmann distribution, 118
Maxwell's equations, 37, 40
mean vector, 509
Mercer's condition, 613
mercury cadmium telluride detector, 278
mercury–neon gas discharge lamp, 420
methane, 158
methanol, 123
Michelson interferometer, 364
midwave infrared, 2
Mie scattering, 76
mixture scatter matrix, 571
mixture-tuned matched filter (MTMF), 678
model-based change detector (MBCD), 710
moderate-resolution atmospheric transmission and radiance code (MODTRAN), 206
modulation depth, 365
modulation transfer function (MTF), 256
molecular decomposition, 122
molecular orbital, 123
monochromator, 419
Morse potential, 112
multiplexer, 266
multispectral imaging, 4

N
negentropy, 521
Neyman–Pearson lemma, 619
Night Vision Imaging Spectrometer (NVIS), 31

nitrous oxide, 158
noise estimation, 519
noise gain factor, 308
noise-adjusted principal-component (NAPC) transformation, 518
noise-equivalent irradiance (NEI), 285
noise-equivalent power (NEP), 285
noise-equivalent radiance (NEL), 294
noise-equivalent reflectance difference NE$\Delta\rho$, 294
noise-equivalent spectral radiance (NESR), 294
noise-equivalent temperature difference ($rmNE\Delta T$), 295
noncentrality parameter, 628, 661
nonlinear dispersion, 340
nonmargin support vector, 592
nonuniformity, 292
normal compositional model (NCM), 553
normal mixture model, 544
normal modes, 120
Normalized Differential Vegetation Index (NDVI), 168
Normalized Image Interpretability Rating Scale (NIIRS), 307
null hypothesis, 617
numerical aperture (NA), 290
Nyquist frequency, 297

O

oblique projection, 497
optical constants, 44
optical depth, 486
optical path difference (OPD), 250, 364
optical system, 247
optical throughput, 290
optical transmission, 264
orthogonal subspace projection (OSP), 670
orthorectification, 698
oscillator strength, 49, 93
ozone, 157

P

P branch, 118
pair-wise adaptive linear matched (PALM) filter, 667
panchromatic imaging, 3
Parzen density, 606
path radiance, 201
pectin, 169
photoconductive gain, 272
photoconductor, 270
photocurrent, 272, 274
photodiode, 272
phycobiliprotein, 165
phytoplankton absorption, 237
Pixel Purity Index^{TM}(PPI^{TM}), 531
plane wave, 39, 42
Plank's constant, 85
plasma frequency, 48
point source, 71
point spread function (PSF), 248
polarization, 47, 79
positivity, 535, 545
potential function, 86
Poynting vector, 54
principal-component analysis (PCA), 510
prior probability, 565
prism, 314
probability density function, 507
probability of detection, 618
probability of false alarm, 618
projection operator, 525
projection vector, 496
pupil-plane radiance, 230
pushbroom scanning, 244

Q

Q branch, 118

quadratic classifier, 566
quadratic spectral filter, 675
quantization noise, 294
quantum detector, 268
quantum efficiency, 269
quantum mechanics, 83
quartz–tungsten (QTH) lamp, 431
quasi-local covariance matrix, 632
quick atmospheric compensation (QUAC), 467

R
R branch, 118
radial wave function, 97
radiance, 70
radiative transfer, 9, 199
radiometric calibration, 423
Rayleigh criterion, 300
Rayleigh scattering, 78
readout integrated circuit (ROIC), 266
readout noise, 292
receiver operating characteristic (ROC), 618
red-edge inflection, 168
red-edge reflectance, 168
reduced mass, 46
Reed–Xiaoli (RX) algorithm, 630
reflectance, 134
reflective spectral region, 201
reflectivity, amplitude, 58
reflectivity, power, 58, 135
relative edge response, 308
relative gain nonuniformity, 427
relative nonlinearity, 429
remote sensing, 1
residual spatial nonuniformity, 428
resolving power, 318
resolving power, Fabry–Perot interferometer, 397
resolving power, Fourier transform spectrometer, 370
resolving power, grating, 326
resolving power, prism, 318
resolving power, spatial Fourier transform spectrometer, 378
resonance frequency, 49
resonant frequency, 47
responsivity, 270
reststrahlen, 175
reststrahlen band, 67

S
Sagnac interferometer, 379
scattering coefficient, 76
scattering cross-section, 73
scattering efficiency, 74
scattering phase function, 74
scene-based calibration, 446
Schrödinger wave equation, 85
score function, 593
search and rescue, 27
separability, 570
separating matrix, 521
shortwave infrared, 2
shot noise, 281
shrinkwrapping, 533
signal spectral radiance, 288
signal-to-clutter ratio (SCR), 622
signal-to-noise ratio (SNR), 284
significance ratio, 684
silicate, 172
silicon detector, 275
Silverstein distribution, 527
simplex maximization, 533
simplex volume, 532
single-facet model, 229
smile, 340
Snell's law, 57
solid angle, 72
spatial noise, 292
spatial position vectors, 39
Spatially Enhanced Broadband Array Spectrograph System (SEBASS), 357

Spatially Modulated Imaging Fourier Transform Spectrometer (SMIFTS), 390
spatial–spectral distortion, 339
specific detectivity, 285
spectral angle, 505
spectral angle mapper (SAM), 648
spectral apparent temperature, 468
spectral calibration, 340, 417
spectral irradiance, 69
spectral matched filter (SMF), 652
spectral measurement vector, 504
spectral mixture, 505
spectral radiance, 71
spectral range, Fabry–Perot interferometer, 397
spectral range, Fourier transform spectrometer, 371
spectral range, grating spectrometer, 326
spectral resolution, 345
spectral resolution, Fourier transform spectrometer, 370
spectral resolution, geometric, 345
spectral response function (SRF), 338
Spectrally Enhanced Broadband Array Spectrograph System (SEBASS), 22
Spectralon®, 431
spectrometer, chromotomographic imaging, 407
spectrometer, Czerny–Turner, 335
spectrometer, double aplanatic prism, 323
spectrometer, Dyson, 337
spectrometer, Fourier transform, 363
spectrometer, grating, 331
spectrometer, Littrow, 322, 334
spectrometer, Offner, 336
spectrometer, Paschen–Runge, 335
spectrometer, prism, 319
spectrometer, Schmidt imaging, 323
spectrometer, wedge imaging, 404
spectroscopy, 8, 95
spectroscopy, rotational, 107
spectroscopy, vibrational, 111
spectrum, 6
specular, 146
speed of light, 39
spherical aberration, 250
spontaneous emission, 91
spot diameter, 254
stationary state, 85
Stefan–Boltzmann law, 153
step-stare pointing, 246
stimulated absorption, 91
stimulated emission, 91
stochastic expectation maximization (SEM), 547, 598
stochastic mixing model (SMM), 551
subpixel replacement model, 676
subspace, 523
subspace model, 524
subsurface reflectance, 236
sulfate, 172
superscribed simplex, 533
supervised classifier, 564
support vector, 591
support vector machine (SVM), 590

T

target subspace, 685
t-distribution, 550
temperature–emissivity separation, 453

transfer calibration, 433
transfer matrix, 143
transimpedance-amplifier circuit, 274
transmission, 55
transmissivity, power, 60
transmittance, 134
true color, 4
two-point radiometric calibration, 425
two-stream method, 136

U
unsupervised classifier, 564
upwelling radiance, 468

V
vegetation, 163
vegetation mapping, 25
vegetation normalization, 458
vegetation science, 25
vibronic, 127
vicarious calibration, 446
virtual dimensionality, 527
visible, 2
volume reflectance, 139

W
wave equation, 38, 42
wave function, 83
wave vector, 39
wavelength, 41
wavenumber, 91
whiskbroom scanning, 244
whitening, 514
Wien displacement law, 153
within-class scatter matrix, 570

X
xenon gas discharge lamp, 420

Z
zero path difference (ZPD), 364

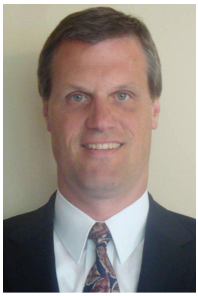

Dr. Michael T. Eismann has more than 25 years of research experience in the fields of electro-optical and infrared technology, hyperspectral remote sensing, and optical information processing. He is currently the Multispectral Sensing and Target Detection Division Technical Advisor at the Sensors Directorate of the Air Force Research Laboratory (AFRL). In this capacity, he is responsible for the technical direction of their electro-optical and infrared research program. Additionally, he serves as an Adjunct Assistant Professor at the Air Force Institute of Technology, Chairman of the Optics Technology Focus Group for the North Atlantic Treaty Organization (NATO) Sensors and Electronics Technology (SET) panel, Associate Editor of SPIE's journal *Optical Engineering*, and is an active participant in multiple professional societies. Prior to joining AFRL in 1996, he was employed by the Environmental Research Institute of Michigan (ERIM), where he was involved in research concerning active and passive optical and infrared targeting and reconnaissance, optical information processing, and holographic optics. He is a Fellow of AFRL, SPIE, and the Military Sensing Symposia (MSS).

Michael was born in Covington, Kentucky in 1964, where he attended high school at the Covington Latin School. He subsequently received a B.S. in Physics from Thomas More College, an M.S. in Electrical Engineering from the Georgia Institute of Technology, and a Ph.D. in Electro-Optics from the University of Dayton. In his free time, Michael is an avid soccer player and enjoys sports of all varieties. He currently lives in Beavercreek, Ohio with his wife Michelle and daughters, Maria and Katie.